Am J Transl Res 2020;12(8):4189-4203
www.ajtr.org /ISSN:1943-8141/AJTR0108920

Original Article

An injectable liposome for sustained release of tanshinone IIA to the treatment of acute blunt muscle injury by augmenting autophagy and alleviating oxidative stress

Jinwu Wang[1,2*], Jie Cai[1,2*], Xingyu Wang[1,2*], Gaosheng Zhu[1,2], Yongzeng Feng[1,2], Hua Chen[1,2#], Leyi Cai[1,2#]

[1]*Department of Orthopaedics, The Second Affiliated Hospital and Yuying Children's Hospital of Wenzhou Medical University, 109 Xue Yuan Xi Road, Wenzhou 325000, Zhejiang, China;* [2]*Wenzhou Medical University, Wenzhou, Zhejiang, China.* [*]*Equal contributors and co-first authors.* [#]*Equal contributors.*

Received February 9, 2020; Accepted July 2, 2020; Epub August 15, 2020; Published August 30, 2020

Abstract: Acute blunt skeletal muscle injury occurs frequently in sports and traffic accidents, and even leads to muscle necrosis and impaired functionality. Current treatment options for muscle injuries remain suboptimal and often result in delayed/incomplete recovery of damaged muscles. Tanshinone IIA is extracted from Salvia Miltiorrhizae, which is effective in the treatment of injury repair. But the clinical application of tanshinone IIA is limited due to its low water solubility, low permeability to biofilm and low bioavailability. In this study, tanshinone IIA liposomes were prepared to improve the bioavailability and sustained release of tanshinone IIA. The particle size, dispersion coefficient, zeta potential, encapsulation efficiency (EE) and drug loading (DL) of tanshinone IIA liposomes were 150.67 ± 27.23 nm, 0.20 ± 0.015, -8.73 ± 2.28 mV, 70.32 ± 4.04% and 15.63%, respectively. The results of quantitative real-time polymerase chain reaction (QRT-PCR) showed that tanshinone IIA liposome significantly promoted the expression of vimentin and reduce MHCIIB expression compared with other groups ($P < 0.05$). Western blotting showed that tanshinone IIA liposome could effectively promote the expression of autophagy-related proteins (VPS34, Beclin 1 and CTSD) and decrease p62 expression levels to treat injured muscle. Through HE, immunohistochemistry, ELISA and serological tests, we found that tanshinone IIA liposome not only effectively promoted the expression of desmin, but also reduced the expression of collagen-I and inhibited the production of pro-inflammatory factors, such as tumor necrosis factor α (TNF-α) and interleukin-6 (IL-6) ($P < 0.05$). In addition, tanshinone IIA liposome therapy significantly reduced the level of malondialdehyde (MDA) and increased the activity of superoxide dismutase (SOD) after muscle injury compared with other groups ($P < 0.05$). In conclusion, tanshinone IIA liposome possesses an effective therapeutic effect on acute blunt muscle injury in rats by augmenting autophagy and alleviating oxidative stress. The continuous release of tanshinone IIA encapsulated by liposomes for disease treatment provide a new idea for the efficient and safe use of drugs with low lipid solubility and bioavailability for the treatment of acute blunt muscle injury and repair of other injuries.

Keywords: Tanshinone IIA, liposome, sustained release, muscle injury

Introduction

Acute blunt injury to skeletal muscle occurs frequently in sports and traffic accidents, and more than 90% of all sports-related injuries to muscle are of the contusion or strain type [1]. According to its severity, muscle injury may be accompanied by capillary rupture, infiltrative hemorrhage, inflammation, oxidative stress, and fibrosis. Muscle injury can lead to a series of pathophysiological changes, such as degeneration, inflammation, regeneration, and the formation of fibrotic tissue, which can occur simultaneously [2, 3]. Without timely and effective treatment, the injury will cause severe pain, and swelling and bruising of the affected muscle, leading to impaired functionality. The treatment of injured muscle follows the RICE principle (rest, ice compression, and elevation) [3] However, the efficacy of compression is controversial. Baldwin *et al*. [4] found that short-term use of non-steroidal anti-inflammatory drugs

(NSAIDs) promotes short-term recovery of muscle function. However, prolonged use of NSAIDs inhibits the proliferation and differentiation of satellite cells, delaying muscle regeneration [5]. Also, NSAIDs have adverse effects on the gastrointestinal tract, kidneys, and heart [5, 6]. Therefore, effective and safe treatment modalities for acute blunt injury to muscle are needed.

Autophagy, a lysosomal-dependent and highly conserved process of macromolecular material circulation in eukaryotic cells, is also essential for cell survival and maintenance under nutrient-deprived conditions [7]. Autophagy induces angiogenesis, reactive oxygen species (ROS) production, and protein kinase B/Akt-mediated activation of bovine aortic endothelial cells, and may be one of the underlying mechanisms of injury repair [8]. In ATP7B-deficient hepatocytes, autophagy is induced in response to copper overload to prevent copper-induced apoptosis [9]. Remote ischemic pretreatment alleviates hepatic ischemia/reperfusion injury (IRI) by activating heme oxygenase-1 (HO-1)/p38 mitogen activated protein kinase-dependent autophagy [10], and bone marrow mesenchymal stem cells activate autophagy via the phosphatidylinositol 3 kinase (PI3K)/Akt signaling pathway, which protects against lung IRI [11]. Thus, injured tissues and organs can be repaired by activating autophagy and reducing apoptosis and oxidative stress.

Tanshinone IIA, a diterpenoid quinone compound, is the major active ingredient of the traditional herbal agent Salvia Miltiorrhizae [12, 13]. Jang *et al*. [14] reported that tanshinone IIA exerts an anti-inflammatory effect by inhibiting activation of the NIK-IKK and MAPK (p38, ERK1/2, JNK) signaling pathways, thereby suppressing liposaccharide (LPS)-induced IκB-α degradation and nuclear factor (NF)-κB activation. Tanshinone IIA also eliminates lipid free radicals and blocks lipid peroxidation [15]. Tanshinone IIA is used for the prevention or treatment of cardiovascular diseases and ischemia-reperfusion injury, and accelerates peripheral nerve regeneration and regulates apoptosis [16, 17]. However, no study has evaluated tanshinone IIA in the treatment of acute blunt-injured muscle. Clinical application of tanshinone IIA is hampered by its poor water solubility, first-pass effect after oral administration, and low bioavailability.

In recent years, liposomes are widely used in various biomedical applications as a targeted and efficient drug delivery [18, 19]. Loading into liposomes can prolong the half-life of a drug *in vivo* and enable its continuous release, thus enhancing its pharmacokinetics and biocompatibility [20]. Yang *et al*. [21] reported that an icariin propylene glycol-liposome suspension increased plasma and tissue icariin concentrations, and increased its biological half-life. In this study, we used the thin-film dispersion method to prepare tanshinone IIA liposome. We aimed to evaluate the therapeutic effects as well as the underlying mechanisms of tanshinone IIA liposomes on acute blunt skeletal muscle injury in rats. There are three novelties in this study. First, we fabricated tanshinone IIA liposomes, which improved its bioavailability and effectively reduced the blood concentration peak valley phenomenon associated with direct drug injection. In turn, this resulted in a relatively stable tanshinone IIA concentration with a lasting effective range, ultimately improving its safety profile. Second, we demonstrated the therapeutic efficacy of tanshinone IIA liposomes in treating acute blunt muscle injury. Lastly, tanshinone IIA alone and tanshinone IIA liposomes were compared, providing insights on the efficacy and safety of drugs with low lipid solubility and bioavailability for the treatment of acute blunt muscle injury and other injuries.

Methods

Materials and reagents

Cholesterol (No. 57-88-5, Shanghai Ivet Medical Technology Co., Ltd, China); Soy lecithin (No. 8002-43-5, Shanghai Ivet Medical Technology Co., Ltd, China); Tanshinone IIA (No. 568-72-9, Sigma Chemical Co., USA); Ethanol (NO. E13-0059, Aladdin Corporation, China); Phosphate-buffered saline (No. P196986, Aladdin Corporation, China); TRIzol reagent (No. 15596018, Invitrogen, USA).

Preparation of tanshinone IIA liposome

We prepared tanshinone IIA liposome by the thin-film dispersion method [22-24]. Briefly, soy lecithin (20 mg), cholesterol (5 mg), and tanshinone IIA (5 mg) were dissolved in chloroform (2 mL) in a round-bottom flask and stirred continuously for 3 minutes. The mixture was evaporat-

ed at 45°C in a rotatory evaporator (RE-52AA; Shanghai Yarong Biochemical Instruments, Shanghai, China) until a homogeneous thin film was observed in the round-bottom flask. In a 37°C water bath, 2 mL of phosphate-buffered saline (PBS, pH 6.4) was added to the round bottom flask to hydrate the tanshinone IIA liposome for 30 minutes. The resulting mixture was homogenized using an ultrasonic cell disruptor (JY98-IIIDN; Ningbo Xinzhi Biotechnology Co., Ltd., Zhejiang, China) at 240 W for 10 minutes (3 s ultrasound at 3 s intervals) on ice, which could effectively avoid excessive temperature during the preparation process. Finally, tanshinone IIA liposome was produced by extruding the solution through a 0.45-μm membrane. Blank liposome was prepared by the same method.

Characterization of tanshinone IIA liposome

Transmission electron microscopy of tanshinone IIA liposome: The morphology of tanshinone IIA liposomes was observed by transmission electron microscopy (TEM; HT7800; Hitachi High Technology Co., Ltd., Tokyo, Japan). One drop of tanshinone IIA liposome suspension was *drip*ped onto a 300-mesh formvar carbon-coated copper grid (No. BZ11033a; Beijing Zhongjingke Instrument Technology Co., Ltd., Beijing, China) for 3 minutes. Next, excess liquid was absorbed using filter paper and the sample was stained with 2% phosphotungstic acid for 3 minutes. Excess liquid was removed with filter paper and the sample was dried at room temperature and observed by TEM.

Particle size, polydispersity index, and zeta potential of tanshinone IIA liposome: A Nano-ZS90 (Malvern Panalytical, Malvern, UK) was used to characterize the particle size, polydispersity index, and zeta potential of the tanshinone IIA liposome at 25°C.

Encapsulation efficiency and drug loading of tanshinone IIA liposome: The encapsulation efficiency (EE) and drug loading (DL) of tanshinone IIA liposome were determined by high-performance liquid chromatography (HPLC) [22, 25] using an Agilent 1260 Infinity II HPLC system, ODS-3 column (4.6 × 150 mm, 5 μm; Agilent, Santa Clara, CA, USA), and C18 precolumn (4.6 × 20 mm; Agilent). The HPLC conditions were as follows: temperature, 25°C; mobile phase, acetonitrile: water (30: 70, v/v); flow rate, 1.0 mL/min; injection volume, 10 μL; and detection wavelength, 270 nm.

At room temperature, the liposome structure was destroyed by mixing 0.5 mL of liposome suspension with 1.5 mL of methanol; subsequently, the total tanshinone IIA content was assayed. Liposomes and free tanshinone IIA were separated by 10 kDa ultrafiltration at 3,000 rpm for 5 minutes, and the free tanshinone IIA content in the ultrafiltrate was determined. The samples were passed through a 0.45-μm syringe filter, and 10 μL was subjected to HPLC. The EE and DL of tanshinone IIA liposome were calculated as follows:

$$EE\ (\%) = (W_T - W_F) \div W_T \times 100\%$$

$$DL\ (\%) = (W_T - W_F) \div W_{NP} \times 100\%$$

Where W_T is the total tanshinone IIA content in a tanshinone IIA liposome sample; W_F is the amount of free tanshinone IIA in a tanshinone IIA liposome sample, and W_{NP} is the weight of nanoparticles.

In vitro release rate of tanshinone IIA liposome: The release of tanshinone IIA from liposomes *in vitro* was determined by the dialysis method and HPLC [23]. Tanshinone IIA liposomes (Tanshinone IIA, ~5 mg) were dissolved in PBS (pH 7.4) and stirred at 400 rpm. After 0.5, 1, 2, 4, 6, 8, 10, 12, and 24 hours, 2 mL of dissolution medium was removed a11nd extruded through a syringe filter (0.45 μm); to maintain the volume, 2 mL of fresh release medium was added. The samples were analyzed by HPLC.

Animals

The Animal Center of the Chinese Academy of Science (Shanghai, China) provided male Sprague-Dawley (SD) rats (250 ± 10 g, n = 32). The rats were maintained in separate cages under constant environmental conditions (22°C, 50 ± 5% relative humidity, 12/12-hour light/dark cycle).

Establishment of a rat model of muscle injury

We established a rat model of skeletal muscle contusion (**Figure 1**). The protocol was approved by the Ethics Committee of Wenzhou Medical University. The rats were anesthetized by intraperitoneal injection of 4% chloral hydrate (0.75 mL/100 g), and the hair of the hind limbs was shaved off. A skeletal muscle contusion was induced by striking the inner part of the right leg (the subcutaneous part was the middle of the gastrocnemius muscle) by a 400 g solid

Figure 1. A: The hairs of the hind legs were shaved off and the gastrocnemius muscles were fully exposed; B: The skeletal muscle contusion was caused by the falling of heavy objects; C: The situation of skeletal muscle contusion. D: The diagram of caudal vein injection.

metal cylinder falling from a height of 67 cm (kinetic energy, 2.63 J). The diameter of the striking surface was 1.0 cm. The rats were divided into four groups of eight rats each using a random number table, as follows: blank model group (5 mL of normal saline injected into the tail vein once daily for 2 weeks), blank liposome group (blank liposome diluted with normal saline and injected into the tail vein once daily for 2 weeks), tanshinone IIA liposome group (20 mg/kg/d; tanshinone IIA liposome diluted with normal saline and injected into the tail vein for 2 weeks), and tanshinone IIA group (20 mg/kg/d; tanshinone IIA in dimethyl sulfoxide diluted 1,000-fold with saline and injected into the tail vein for 2 weeks). We determined the dosage of tanshinone IIA for injection based on a previously published study [25]. On days 7 and 14 after muscle injury, four rats per group, selected at random, were euthanized and their right gastrocnemius muscle was harvested.

Quantitative real-time polymerase chain reaction

The effect of tanshinone IIA liposome on MHCIIB and vimentin expression was evaluated by quantitative real-time polymerase chain reaction (qRT-PCR) [26, 27]. The housekeeping gene glyceraldehyde-3-phosphate dehydrogenase (GAPDH) was used as the reference for normalization. Briefly, total RNA was extracted from the gastrocnemius muscle using TRIzol reagent (15596018; Invitrogen, Carlsbad, CA, USA) according to the manufacturer's instructions. The concentration and purity of the RNA were analyzed spectrophotometrically at 260 nm using a Nanodrop 2000 (Thermo, Waltham, MA, USA). The RNA concentration was adjusted to 200 ng/μL by dilution. cDNA was synthesized from the RNA by reverse transcription using the Thermo Scientific Revert-Aid RT Kit (WG441-K1622; Thermo) according to the manufacturer's instructions. Subsequently, qRT-PCR was performed using a SLAN Fluorescence Quantitative PCR Detection System (Shanghai Hongshi Medical Devices Co., Ltd., Shanghai, China). Each 25-μL qRT-PCR reaction comprised 12.5 μL of 2 × qPCR Mix, 2.0 μL of 7.5 μM primers, 2.5 μL of reverse transcription product, and 8.0 μL of ddH_2O. The samples underwent 40 cycles of initial denaturation at 95°C for 10 min, denaturation at 95°C for 15 s, and annealing at 60°C for 60 s in triplicate. The primer sequences are listed in **Table 1**.

Western blotting

The rats were euthanized on day 14 after muscle injury. Samples (0.5 × 0.5 cm) from the middle of injured muscles (n = 4) were harvested and stored at -80°C. After degrading the muscle tissue in lysis buffer, the protein concentration was measured by bicinchoninic acid assay. Sixty grams of protein were separated by electrophoresis in 12% (w/v) gels and transferred to polyvinylidene difluoride membranes (Roche Applied Science, Indianapolis, IN, USA). After blocking with 5% (w/v) nonfat milk for 2 hours at room temperature, the membranes were incubated with the following primary antibodies at 4°C overnight: VPS34 (1:1,000 dilution), beclin 1 (1:1,000), CTSD (1:1,000), p62 (1:1,000), and GAPDH (1:1,000). Next, the

Table 1. Primer sequence for use in reverse transcription-quantitative polymerase chain reaction

Genes	Sequence (5'-3')	Primer length (bp)	Product length (bp)	Annealing (°C)
MHCIIB F	CTGATCACCACCAACCCATAT	20	419	58.03
MHCIIB R	GTGACCATCCACAGGAACATC	21		
Vimentin F	CAAGAACACCCGCACCAA	17	180	58.32
Vimentin R	TCCCTCATCTCCTCCTCGTA	20		
GAPDH F	GCAAGTTCAACGGCACAG	18	141	58.6
GAPDH R	CGCCAGTAGACTCCACGAC	18		

membranes were incubated with horseradish peroxidase (HRP)-conjugated secondary IgG (1:5,000) for 2 h at room temperature, and protein bands were visualized using the ECL Plus Reagent Kit (Amersham Biosciences, Little Chalfont, UK). Band intensity was quantified with Image Lab 3.0 software (Bio-Rad, Hercules, CA, USA).

Histological analysis

Muscle tissues were harvested at predetermined times and fixed in 4% paraformaldehyde solution for 24 hours at room temperature. Next, the tissue samples were dehydrated in an ethanol gradient (75%, 85%, 95%, and 100%), cleared with dimethylbenzene, and embedded in paraffin blocks at 65°C. Serial transverse sections (4-μm-thick) were stained with hematoxylin and eosin (HE) and observed and imaged under a microscope (Cx23; Olympus Corp., Tokyo, Japan) at 400 × magnification.

Immunohistochemical staining

Immunohistochemical (IHC) staining was performed to determine the expression levels of desmin, collagen I, and tumor necrosis factor (TNF)-α at predetermined times after muscle injury. The sections were dewaxed with xylene and rehydrated in a series of concentrations of ethanol. After rinsing in pure water, the sections were placed in citrate antigen repair buffer (pH 6.0). To block endogenous peroxidase activity, the sections were transferred to 3% H_2O_2 and incubated in darkness for 25 minutes at room temperature, followed by three washes with PBS (pH 7.4) for 5 minutes each. Next, bovine serum albumin (BSA; 3%) was added to cover the tissues, and the sections was sealed at room temperature for 30 minutes. The sealing solution was shaken off gently. After adding a certain proportion of the primary antibody (anti-desmin rabbit pAb [GB11081], 1:200; anti-collagen I rabbit pAb [GB11022-3], 1:500; anti-TNF-α mouse mAb [GB13188-2], 1:200; all Servicebio, Woburn, MA, USA), the sections were incubated overnight in a wet box at 4°C. On the following day, the sections were washed with PBS (pH 7.4) three times for 5 minutes each. The sections were dried, and HRP-conjugated secondary antibodies of the appropriate species/genera were added, followed by incubation at room temperature for 50 minutes.

After reaction with DAB substrate and counterstaining with hematoxylin, the areas positive for desmin, collagen I, and TNF-α were visualized under a microscope (Cx23; Olympus Corp.). The integrated optical densities (IODs) and pixel areas of corresponding tissue (AREAs) of desmin, collagen I, and TNF-α in injured muscle were analyzed using Image Pro Plus 6.0 (Media Cybernetics, Inc., Silver Spring, MD, USA). The average optical density (AOD) was calculated as: AOD = IOD ÷ AREA (3).

Assay of the malondialdehyde level and superoxide dismutase activity

Four rats per group were euthanized at 7 and 14 days postoperatively, and the skin fascia was immediately cut into layers at the gastrocnemius. Several pieces of injured gastrocnemius muscle tissue were removed, washed in normal saline at 4°C, and dried with filter paper. The muscle pieces were weighed, and homogenates were prepared by adding 1:10 w/v saline (4°C) and centrifuging at 4,000 rpm at 4°C for 10 minutes. The content of malondialdehyde (MDA) and activity of superoxide dismutase (SOD) in the supernatant were determined by the thiobarbituric acid method and enzymatic xanthine oxidase assay, respectively [28, 29].

Estimation of IL-6 and TNF-α levels

On days 7 and 14 after muscle injury, the serum interleukin (IL)-6 and TNF-α levels were determined using commercial enzyme-linked immu-

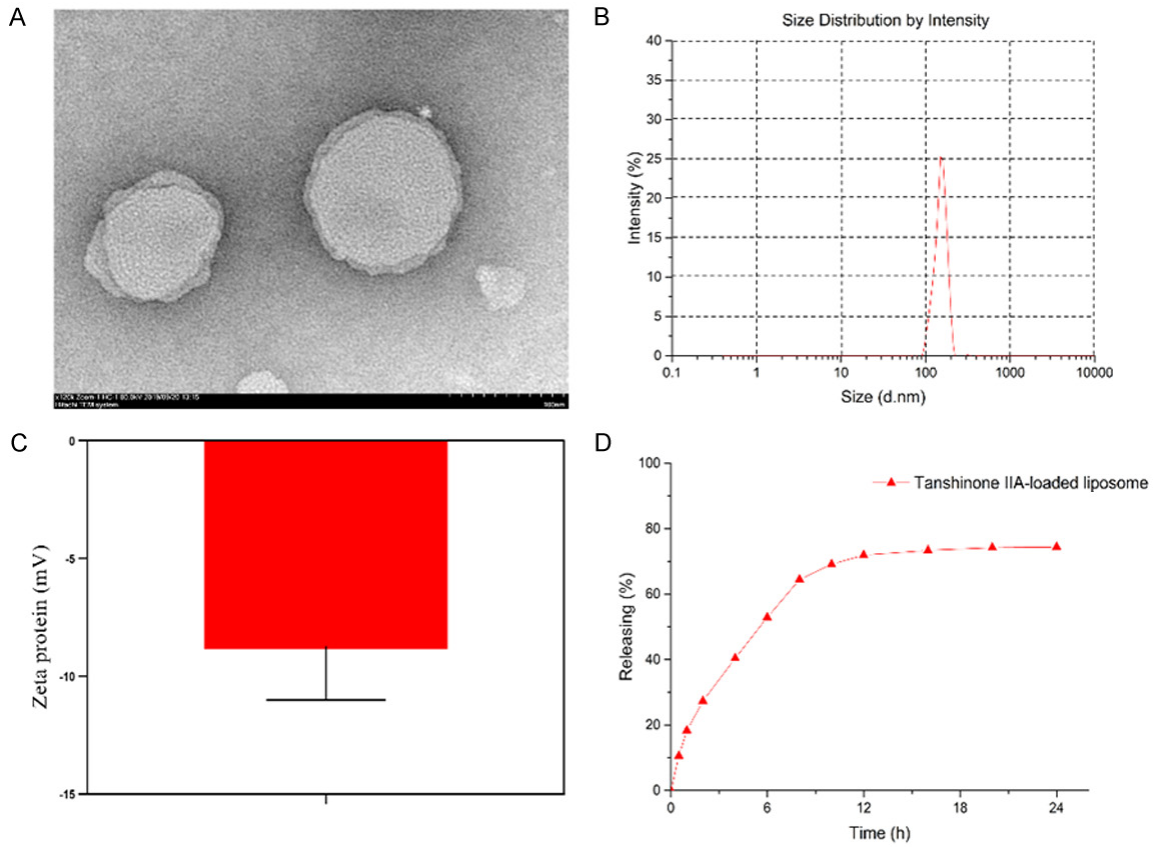

Figure 2. Characterization of tanshinone IIA liposome. A: The structure of tanshinone IIA liposome was observed by transmission electron microscope; B: The size of the tanshinone IIA liposome; C: Zeta potential of tanshinone IIA liposome; D: Release rate of tanshinone IIA liposome.

nosorbent assay (ELISA) kits according to the manufacturers' protocols.

Statistical analysis

Results are expressed as means ± SD. SPSS software (version 24.0; IBM Corp., Armonk, NY, USA) was used to conduct the statistical analysis. One-way analysis of variance was performed to evaluate differences among multiple groups. GraphPad Prism software (version 7.0: GraphPad Software Inc., La Jolla, CA, USA) was used to construct graphs. *P*-values < 0.05 were considered significant.

Results

Characteristics of tanshinone IIA liposome

By TEM, tanshinone IIA liposomes were shown to be small, single-chamber spherical vesicles, which were relatively homogeneous in size (**Figure 2A**). The particle size, dispersion coefficient, and zeta potential of the tanshinone IIA liposomes were 150.67 ± 27.23 nm, 0.20 ± 0.015, and -8.73 ± 2.28 mV, respectively (**Figure 2B** and **2C**). The EE of tanshinone IIA liposome was 70.32 ± 4.04% and the DL rate was 15.63%. As illustrated in **Figure 2D**, tanshinone IIA liposomes showed sustained drug release *in vitro*.

Tanshinone IIA liposome modulated the expression of MHCIIB and vimentin

By qRT-PCR, there was no significant difference between the blank model and blank liposome groups in MHCIIB or vimentin expression on days 7 and 14 (P > 0.05; **Figure 3**). Tanshinone IIA increased the expression of vimentin and reduced that of MHCIIB on days 7 and 14 (P < 0.05; **Figure 3**). Compared with the tanshinone IIA group, the expression of vimentin (1.60 ± 0.17 and 1.27 ± 0.06, respectively) was significantly increased and that of MHCIIB (0.32 ± 0.02 and 0.18 ± 0.02, respectively) was

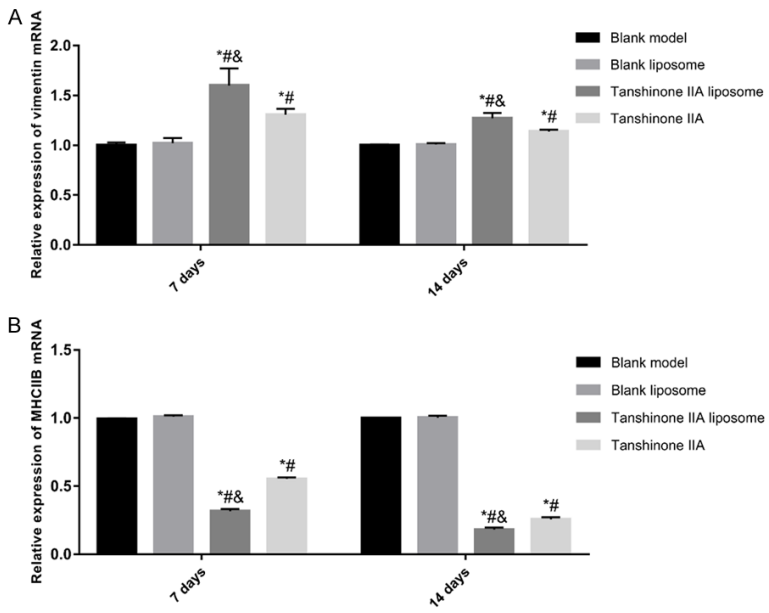

Figure 3. Tanshinone IIA liposome promoted the expression of the MHCIIB and vimentin at 7 and 14 days after muscle injury. A: The expression of MHCIIB in different experimental groups at 7 and 14 days after muscle injury; B: The expression of vimentin in different experimental groups at 7 and 14 days after muscle injury. Data are mean ± standard error, n = 4 per group. * represents a comparison with blank model group, $P < 0.05$; # represents a comparison with blank liposome group, $P < 0.05$; & represents a comparison with tanshinone IIA group, $P < 0.05$.

decreased, in the tanshinone IIA liposome group on days 7 and 14 after muscle injury ($P < 0.05$; **Figure 3**).

Tanshinone IIA liposome upregulates autophagy in injured muscle

VPS34 and Beclin 1 are localized to the preautophagosomal structure, CTSD is a marker of autolysosomes, and p62 reflects autophagic degradation. Hence, we performed western blotting of the beclin 1, VPS34, CTSD, and p62 levels in injured muscle (**Figure 4**). The VPS34, beclin 1, and CTSD levels were highest, and the p62 level was lowest, in the tanshinone IIA liposome group (**Figure 4**; $P < 0.05$). Tanshinone IIA increased the levels of vps34, beclin 1, and CTSD compared with the blank model and blank liposome groups (**Figure 4**; $P < 0.05$). The levels of autophagy-related proteins (VPS34, beclin 1, CTSD and p62) were not significantly different between the blank model and blank liposome groups ($P > 0.05$).

Histological analysis and IHC staining

On day 7, but not on day 14, some degree of gastrocnemius surface edema was observed in all groups. As shown in **Figure 5A**, on day 7, a large number of muscle cells in the blank model and blank liposome groups exhibited swelling, necrosis, dissolution, fibrosis, atrophy, and inflammatory cell infiltration. Compared with the blank model group, inflammatory cell infiltration and fibrosis were reduced in the tanshinone IIA group. Furthermore, in the tanshinone IIA liposome group, the regenerated muscle fibers were arranged in an orderly fashion, the cells had a slender nucleus, the number of fibrocytes was increased, and the number of infiltrating inflammatory cells was decreased; moreover, there was no swelling or necrosis of muscle cells and no scarring. On day 14, a small number of regenerated intact muscle fibers were found in the tanshinone IIA liposome group; there were no inflammatory cells and a small number of new blood vessels were observed, indicating recovery from injury. The cells in the tanshinone IIA group were compact and some fibrosis and inflammatory cell infiltration were evident. However, there was only slight improvement in the muscles in the blank model and blank liposome groups; moreover, muscle atrophy, inflammatory cell infiltration, and massive fibrosis remained evident on day 14 in those groups.

IHC staining showed that the desmin level was higher in the tanshinone IIA liposome group (2.06 ± 0.28 and 1.87 ± 0.03, respectively) compared with the tanshinone IIA group (1.54 ± 0.19 and 1.49 ± 0.18, respectively) on days 7 and 14 (**Figure 5B**; $P < 0.05$). Also, the expression levels of collagen 1 (0.56 ± 0.07 and 0.63 ± 0.03, respectively) (**Figure 6A**) and TNF-α (0.66 ± 0.02 and 0.29 ± 0.02, respectively) (**Figure 6B**) were lower in the tanshinone IIA liposome group on days 7 and 14 after acute blunt muscle injury ($P < 0.05$). Importantly, there was no difference in desmin, collagen-1, or TNF-α expression between the blank model and blank liposome groups on days 7 and 14,

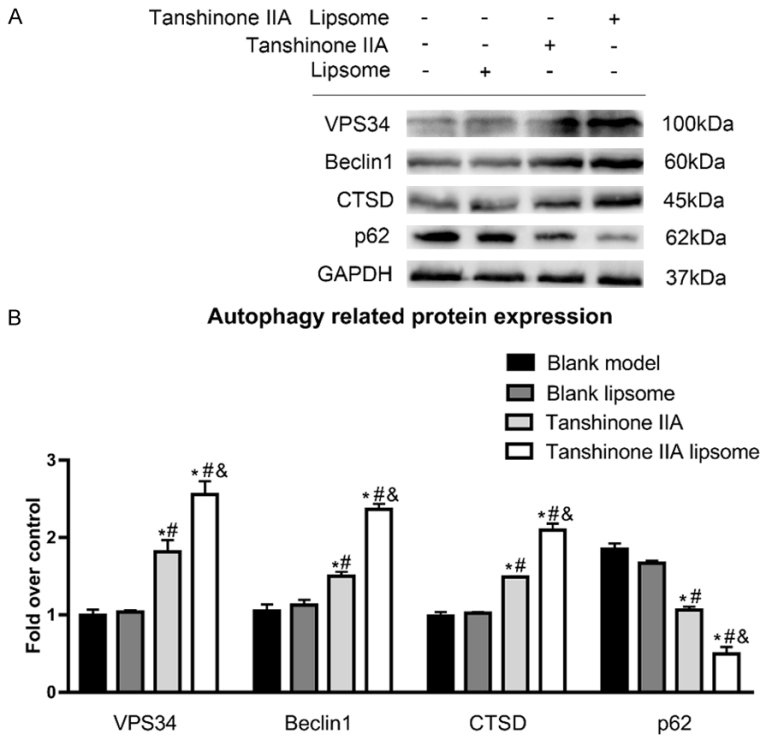

Figure 4. A: Western blotting for VPS34, Beclin 1, CTSD and p62 expression in the muscle injury of all groups. Gels were electrophoresed under the same experimental conditions, and cropped blots are shown here. B: Histograms of optical density values for VPS34, Beclin 1, CTSD and p62 as calculated by Western blotting. Data are mean ± standard error, n = 4 per group. + stands for giving the corresponding stimulus and - stands for no interference. * represents a comparison with blank model group, P < 0.05; # represents a comparison with blank liposome group, P < 0.05; & represents a comparison with tanshinone IIA group, P < 0.05.

indicating biocompatibility of the liposomes (P > 0.05, **Figures 5B** and **6**).

Effect of tanshinone IIA liposome on oxidative stress

The MDA level and SOD activity are shown in **Figure 7A** and **7B**. Compared with the blank model group and blank liposome group, the MDA content in the tanshinone IIA liposome group (3.11 ± 0.05 and 2.10 ± 0.33 nmol·mg^{-1}·protein^{-1}, respectively) and tanshinone IIA group (4.55 ± 0.062 and 3.51 ± 0.40 nmol·mg^{-1}·protein^{-1}, respectively) decreased significantly on days 7 and 14 (P < 0.05), and the MDA content in the tanshinone IIA liposome group was significantly lower than that in the tanshinone IIA group (P < 0.05). On days 7 and 14, the SOD activity in the tanshinone IIA liposome group (72.50 ± 2.08 and 83.98 ± 0.86 u.mg^{-1}·protein^{-1}, respectively) and tanshinone IIA group (64.25 ± 2.22 and 71.25 ± 2.22 u.mg^{-1}·protein^{-1}, respectively) increased significantly, and the increase was greater in the tanshinone IIA liposome group (P < 0.05). However, there was no significant difference in MDA content or SOD activity between the blank model group and blank liposome group (P > 0.05).

Effect of tanshinone IIA liposome on the levels of proinflammatory cytokines

Next, we assayed the levels of the proinflammatory cytokines TNF-α and IL-6. Compared with the blank model and blank liposome groups, the TNF-α and IL-6 levels were significantly decreased in the tanshinone IIA liposome and tanshinone IIA groups (**Figure 7C** and **7D**; P < 0.05). Also, tanshinone IIA liposome (TNF-α: 52.25 ± 7.85 and 35.05 ± 3.63 pg/mL; IL-6: 65.75 ± 6.60 and 46.50 ± 3.11 pg/mL, respectively) exerted a significantly greater anti-inflammatory effect than tanshinone IIA (TNF-α: 77.00 ± 2.45 and 62.88 ± 5.78 pg/mL; IL-6: 91.25 ± 2.22 and 67.00 ± 4.24 pg/mL, respectively) on days 7 and 14 after acute blunt muscle injury. Notably, the TNF-α and IL-6 levels were similar between the blank model and blank liposome groups (**Figure 7C** and **7D**; P > 0.05). Therefore, the anti-inflammatory effect of tanshinone IIA was increased by its encapsulation in liposomes.

Discussion

Tanshinone IIA, the main ingredient of the Chinese medicine Salvia Miltiorrhizae, has anti-inflammatory, antifibrotic, and antioxidant activity, regulates apoptosis, and is used in the treatment of ischemia-reperfusion and other types of injury [30-33]. However, the clinical utility of tanshinone IIA is limited by its low water solubility, biofilm permeation, and bioavailability. In this study, tanshinone IIA was

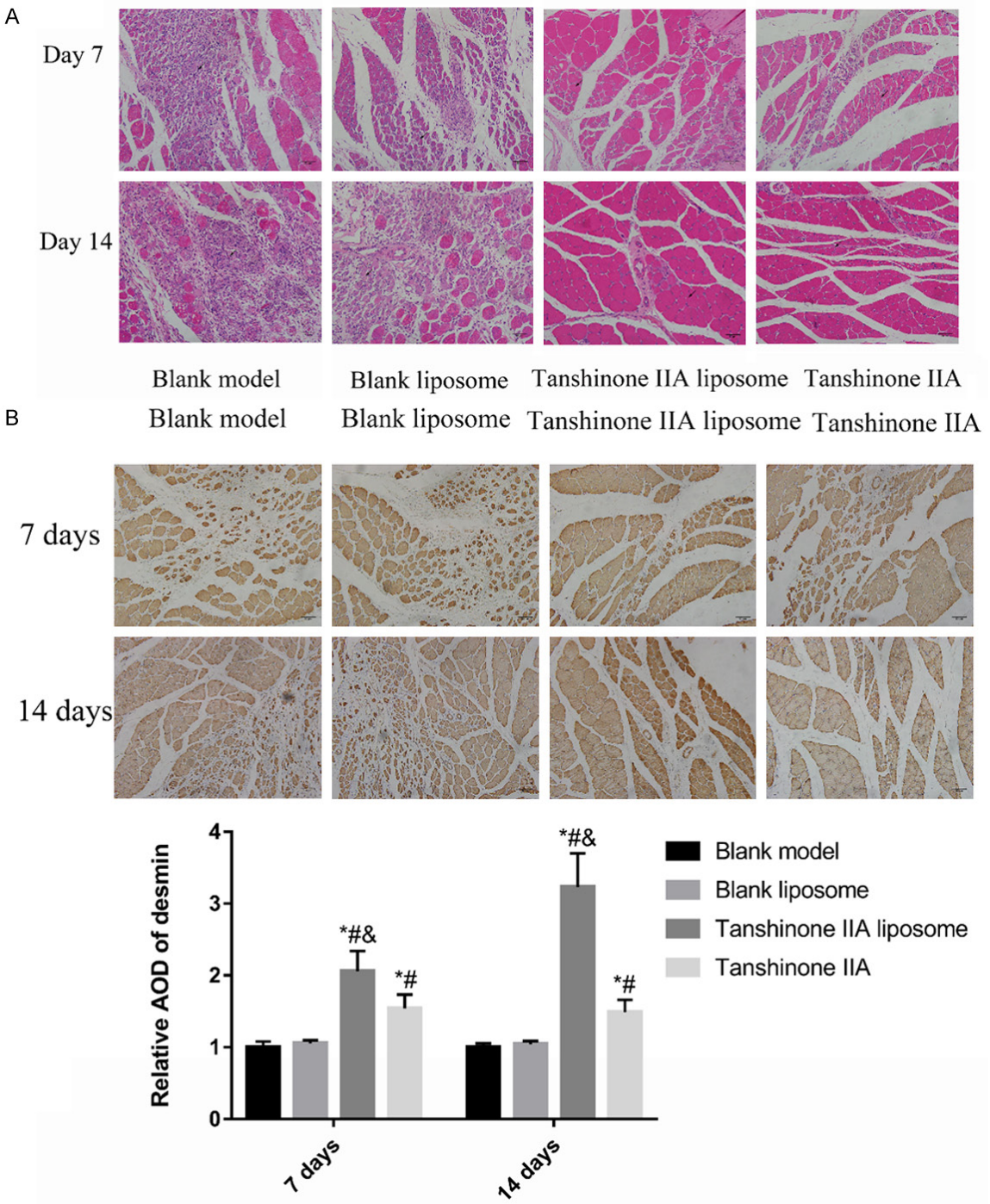

Figure 5. A: Hematoxylin and eosin (HE) -stained of the injured muscle in each group (original magnification ×200; scale bar, 50 μm); B: Immunohistochemistry (IHC) of proteins desmin in injured muscle (original magnification, ×200; scan bar, 50 μm) and the quantification of average optical density of desmin in IHC in each group. Data are mean ± standard error, n = 4 per group. * represents a comparison with blank model group, $P < 0.05$; # represents a comparison with blank liposome group, $P < 0.05$; & represents a comparison with tanshinone IIA group, $P < 0.05$.

transformed into tanshinone IIA liposome to improve its bioavailability. We evaluated the release and therapeutic efficacy of tanshinone IIA liposome, as well as the underlying mechanisms, in a rat model of acute blunt-injured muscle.

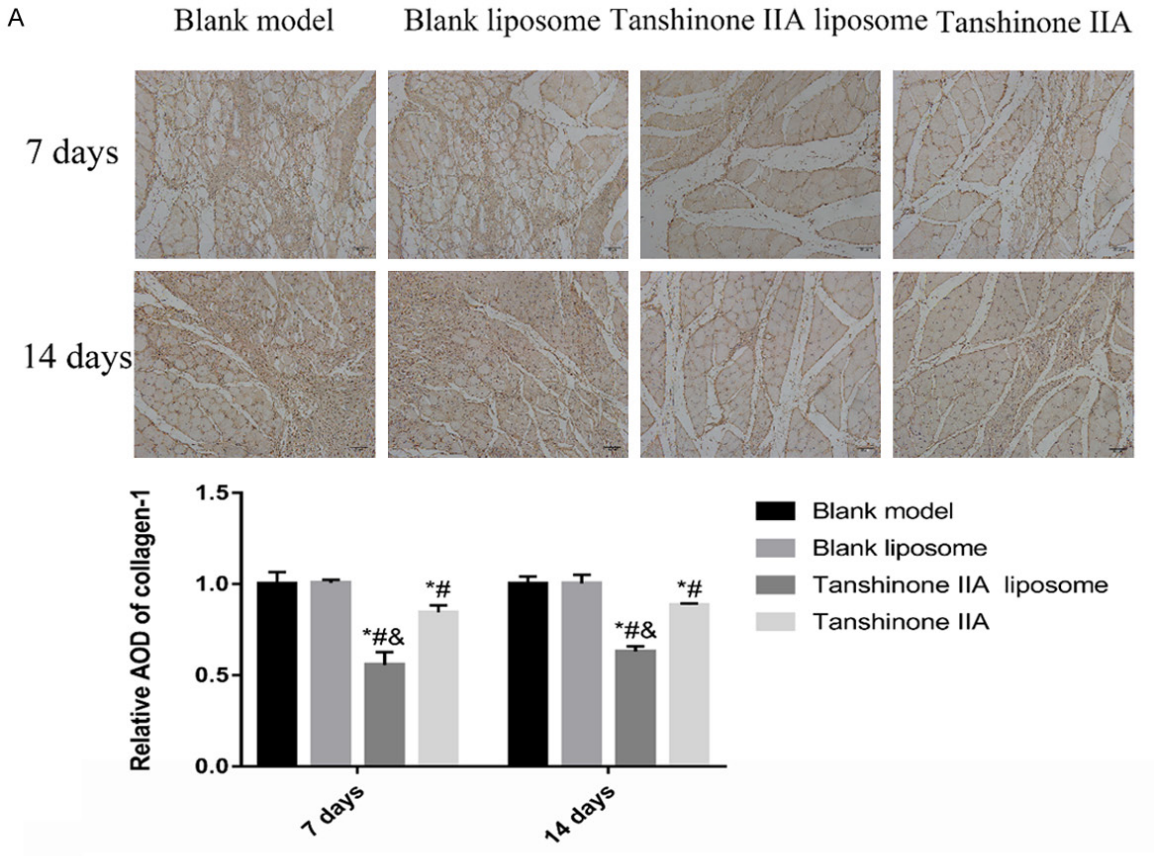
A
Blank model
Blank liposome
Tanshinone IIA liposome
Tanshinone IIA
7 days
14 days
Relative AOD of collagen-1
1.5
1.0
0.5
0.0
*#&
*#
*#&
*#
7 days
14 days
Blank model
Blank liposome
Tanshinone IIA liposome
Tanshinone IIA

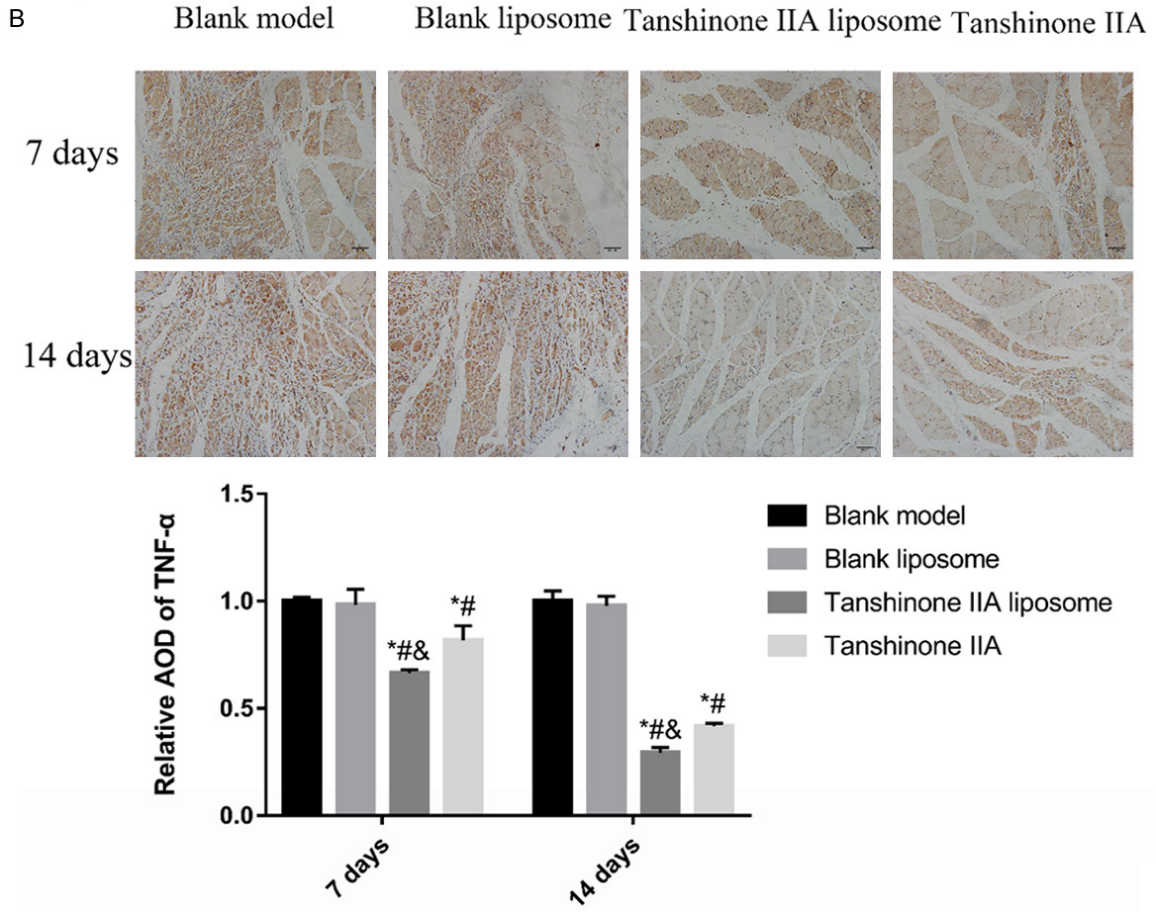
B
Blank model
Blank liposome
Tanshinone IIA liposome
Tanshinone IIA
7 days
14 days
Relative AOD of TNF-α
1.5
1.0
0.5
0.0
*#&
*#
*#&
*#
7 days
14 days
Blank model
Blank liposome
Tanshinone IIA liposome
Tanshinone IIA

Figure 6. A: Collagen I level in the muscle from each group by immunohistochemistry (IHC) (original magnification ×200; scale bar, 50 μm). And the histograms of average optical density for collagen I by IHC in each group; B: The TNF-α expression in the muscle from each group by immunohistochemistry (IHC) (original magnification ×200; scale bar, 50 μm). And the histograms of average optical density for collagen I by IHC in each group. Data are mean ± standard error, n = 4 per group. * represents a comparison with blank model group, P<0.05; # represents a comparison with blank liposome group, P < 0.05; & represents a comparison with tanshinone IIA group, P < 0.05.

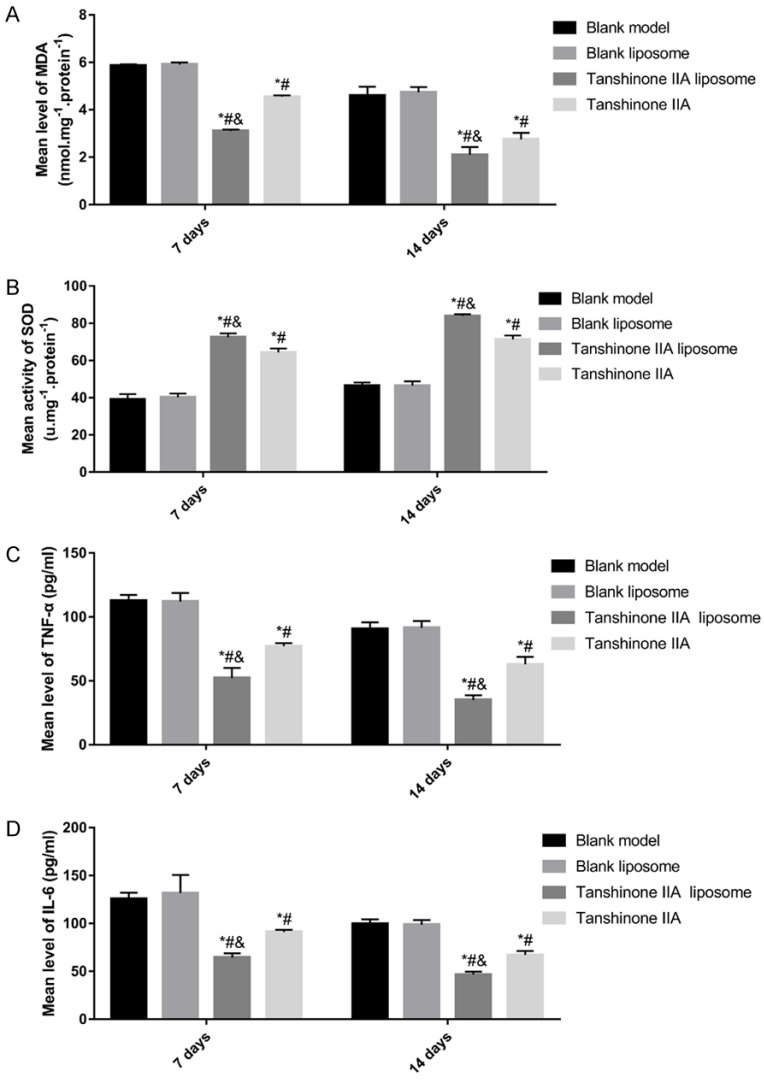

Figure 7. Effects of tanshinone IIA liposome on proinflammatory cytokines. A: MDA level in each group was gauged through an approach triggered by a reaction with thiobarbituric acid. B: SOD activity in each group was measured by the oxidase enzymatic method. C and D: TNF-α and IL-6 expression was detected by ELISAs. Data are mean ± standard error, n = 4 per group. * represents a comparison with blank model group, P < 0.05; # represents a comparison with blank liposome group, P < 0.05; & represents a comparison with tanshinone IIA group, P < 0.05.

The particle size, dispersion coefficient, and zeta potential of tanshinone IIA liposomes prepared by the thin-film dispersion method were 150.67 ± 27.23 nm, 0.20 ± 0.015 and -8.73 ± 2.28 mV, respectively; the liposomes spherical in shape. The EE of tanshinone IIA liposome was 70.32 ± 4.04% and its DL rate was 15.63%. However, there were differences between tanshinone IIA liposomes and artesunate liposomes [22]. Those differences likely resulted from our improvements to the preparation method. We performed ultrasonic dispersion at 240 W and used a 0.45-mm, rather than a 0.22-mm, microporous membrane to extrude the liposomes, with the aim of preventing excessive temperature and obtaining smaller and more uniform liposomes. Most of the liposomes were uniformly dispersed, but some aggregates were present, possibly because of their low zeta potential. A higher zeta potential (> 30 mV) increases liposomal stability and dispersion [24, 34] by increasing their electrostatic repulsion. Indeed, Feng *et al*. [27] reported that the zeta potential of resveratrol liposomes was -30 mV, and the liposomes were dispersed uniformly and stably. The zeta potential of tanshinone IIA liposome was -8.73 ± 2.28 mV, suggesting insufficient electrostatic repulsion. Tanshinone IIA liposome showed burst release for 8 hours (release rate, 64.46%); the cumulative release rate after 24 hours was 74.35%, indicating that tanshinone IIA liposome has good sustained-release properties. Sustained release can reduce the peaks and valleys in blood concentration, i.e., can maintain the

blood concentration of tanshinone IIA in the effective range and thus improve its safety. This preparation method is suitable only for liposoluble drugs. According to differences in physicochemical properties, such as solubility, preparation conditions can also be adjusted to achieve the best DL and EE.

Autophagy refers to self-catabolism of damaged or dysfunctional cellular components, which are recycled to provide nutrients. Autophagy promotes cell survival during nutrient deprivation or stress, prevents neurodegeneration, and degrades invading microorganisms and intracellular antigens [7]. Therefore, autophagy plays an important role in injury repair. Autophagy involves formation of the autophagosome, which fuses with the lysosome and thus leads to digestion of the substrate. Consequently, we analyzed the levels of Beclin 1 and VPS34 (markers of autophagosomes), CTSD (marker of autolysosomes), and p62 (marker of autophagic degradation). Western blotting showed that the expression of Beclin 1 and VPS34 was highest in the tanshinone IIA liposome group, suggesting greater autophagosome formation. Furthermore, CTSD and p62 expression levels were increased and decreased respectively by tanshinone IIA liposome, indicating increased autophagic flux. These results suggest that tanshinone IIA liposome repairs injured muscle by upregulating autophagy, which provide strong evidence of tanshinone IIA liposome's therapeutic benefit for acute blunt muscle injury with novel mechanistic insight, highlighting tanshinone IIA liposome's potential for clinical application.

HE staining showed that tanshinone IIA liposome regenerated and maintained the structure of muscle fibers, reduced inflammatory cell infiltration, induced slight neovascularization, and restored the morphology of muscle cells; these are all signs of recovery of the injured muscle. Tanshinone IIA also repaired injured muscle to some extent, albeit that this was accompanied by a degree of inflammatory cell infiltration and fibrosis. MHCIIB controls the immune response; regulates the division, proliferation, and interactions of lymphocytes; and affects the repair of injured skeletal muscle [35]. In this study, both tanshinone IIA and tanshinone IIA liposomes reduced the expression of MHCIIB. This may have been due to repair of injured muscle cells and surrounding cells. By contrast, the expression of vimentin was increased by tanshinone IIA liposome and tanshinone IIA. Vimentin, a marker of recovery of injured muscle, is related to cytoskeletal and cellular integrity [27, 36]. The expression of vimentin was increased more by tanshinone IIA liposome compared with tanshinone IIA, suggesting that the former promoted greater and longer-lasting recovery of acute blunt-injured muscle. However, further research is needed to determine the underlying mechanism.

Desmin is an intermediate filament protein that connects the Z-line with mitochondria, the cell membrane and the cell nucleus. Desmin also prevents excessive sarcomere involvement in muscle contraction and relaxation [37]. Loss of desmin is a morphological index of skeletal muscle injury [38]. Type I collagen is one of the major types of collagen in muscle tissue. Gaps in injured muscle are initially filled by hematoma, and excessive production of collagen hinders muscle repair and regeneration [39]. IHC staining showed that that tanshinone IIA liposome facilitated muscle recovery by increasing the expression of desmin and reducing that of collagen I. Similarly, Criswell *et al*. reported that high desmin expression stabilizes organelles and maintains the morphology of muscle fibers, thereby promoting their rapid recovery [40]. Collagen I exerts the opposite effects in injured muscle [41]. Thus, we initially assumed that tanshinone IIA liposomes regulate the expression of desmin and collagen I to promote skeletal muscle repair.

Repair of injured skeletal muscle involves multiple inflammatory mediators, cytokines, and hormones [42]. Inflammation plays a key role in muscle repair because proinflammatory cytokines modulate the cellular environment, which controls other repair processes [43]. TNF-α, a proinflammatory factor, plays an important role in the inflammatory response, injury repair, and cell differentiation; it also activates the inflammatory cascade and induces the release of IL-6 to repair injured muscle. However, excessive inflammatory stimulation inhibits muscle repair. IHC staining showed that tanshinone IIA reduced excessive expression of TNF-α in injured skeletal muscle and prevented injury to fine muscle afferents, which is closely related to the recovery of muscle function. Also, the anti-inflammatory effect of tanshinone IIA liposome was greater than that of tanshinone IIA.

The plasma TNF-α and IL-6 levels at 7 and 14 days after injury confirmed the IHC results. The anti-inflammatory effect of tanshinone IIA liposome prevented secondary inflammatory injury to muscle and accelerated muscle repair.

After muscle injury, the sarcolemma and basement membrane are destroyed, leading to neutrophil and macrophage infiltration and activation, and the generation of reduced nicotinamide adenine dinucleotide phosphate oxidase complex. That complex facilitates the formation of superoxide ions and oxygen free radicals, causing further damage to skeletal muscle [44]. MDA, a product of lipid peroxidation, is used to measure the intensity of free radical reactions. Its content reflects the rate and intensity of lipid peroxidation, and indirectly reflects the degree of skeletal muscle injury and lipid peroxidation [45]. SOD is the main antioxidant enzyme in skeletal muscle, wherein it eliminates free radicals and peroxides to protect against oxidative stress and promote tissue repair [46, 47]. Thus, the level of MDA and activity of SOD are important biomarkers of oxidative stress. In this study, tanshinone IIA liposome significantly reduced the MDA level and increased SOD activity after skeletal muscle injury. Also, tanshinone IIA liposome enhanced the endogenous antioxidant capacity, reduced the levels of lipid peroxidation products and free radicals, and ameliorated the cell-membrane damage caused by oxygen free radicals. Similarly, Wang *et al*. found that inhibition of oxidative stress protected normal tissues and cells from secondary injury [48].

Tanshinone IIA promoted the repair of acute blunt-injured skeletal muscle by augmenting autophagy, reducing inflammation and oxidative stress, modulating vimentin and desmin expression, and repairing the damaged cytoskeleton. Tanshinone IIA liposome exerted a greater therapeutic effect than tanshinone IIA by maintaining the plasma tanshinone IIA concentration, thereby improving its safety and bioavailability.

Conclusion

Liposomal encapsulation of tanshinone IIA reduced peaks and valleys in plasma concentration after direct injection, maintained the plasma tanshinone IIA concentration, and improved the safety and bioavailability of tanshinone IIA. In addition, tanshinone IIA liposome ameliorated acute blunt gastrocnemius injury in rats by augmenting autophagy, reducing inflammation, alleviating oxidative stress, modulating the expression of vimentin and desmin, and repairing the damaged cytoskeleton. Therefore, liposomally encapsulated tanshinone IIA has potential for the treatment of acute blunt-injured muscle.

Acknowledgements

This study was supported by the Zhejiang Medical and Health Science and Technology Plan Project (No. 2017KY480) and National Natural Science Foundation of China (No. 81701928).

Disclosure of conflict of interest

None.

Abbreviations

PBS, phosphate-buffered saline; TEM, transmission electron microscope; PDI, polydispersity index; EE, Encapsulation efficiency; DL, drug loading; HPLC, high performance liquid chromatography; SD, Sprague-Dawley; QRT-PCR, Quantitative real-time polymerase chain reaction; CTSD, cathepsin D; GAPDH, glyceraldehyde-3-phosphate dehydrogenase; IHC, Immunohistochemical staining; BSA, bovine serum albumin; IOD, integrated optical density; AOD, average optical density; MDA, malondialdehyde; SOD, superoxide dismutase.

Address correspondence to: Dr. Leyi Cai, Department of Orthopaedics, The Second Affiliated Hospital and Yuying Children's Hospital of Wenzhou Medical University, 109 Xue Yuan Xi Road, Wenzhou 325000, Zhejiang, China. Tel: +86-15088556021; Fax: +86-0577-88002810; E-mail: caileyi@wmu.edu.cn

References

[1] Fanchini M, Steendahl IB, Impellizzeri FM, Pruna R, Dupont G, Coutts AJ, Meyer T and McCall A. Exercise-based strategies to prevent muscle injury in elite footballers: a systematic review and best evidence synthesis. Sports Med 2020; [Epub ahead of print].

[2] Chazaud B. Inflammation and skeletal muscle regeneration: leave it to the macrophages! Trends Immunol 2020; 41: 481-492.

[3] Jarvinen TA, Jarvinen TL, Kaariainen M, Kalimo H and Jarvinen M. Muscle injuries: biology and treatment. Am J Sports Med 2005; 33: 745-764.

[4] Baldwin Lanier A. Use of nonsteroidal anti-inflammatory drugs following exercise-induced muscle injury. Sports Med 2003; 33: 177-185.
[5] Morelli KM, Brown LB and Warren GL. Effect of NSAIDs on recovery from acute skeletal muscle injury: a systematic review and meta-analysis. Am J Sports Med 2018; 46: 224-233.
[6] Langendorf EK, Klein A, Drees P, Rommens PM, Mattyasovszky SG and Ritz U. Exposure to radial extracorporeal shockwaves induces muscle regeneration after muscle injury in a surgical rat model. J Orthop Res 2020; 38: 1386-1397.
[7] Parzych KR and Klionsky DJ. An overview of autophagy: morphology, mechanism, and regulation. Antioxid Redox Signal 2014; 20: 460-473.
[8] Yu L, Chen Y and Tooze SA. Autophagy pathway: cellular and molecular mechanisms. Autophagy 2018; 14: 207-215.
[9] Polishchuk EV, Merolla A, Lichtmannegger J, Romano A, Indrieri A, Ilyechova EY, Concilli M, De Cegli R, Crispino R, Mariniello M, Petruzzelli R, Ranucci G, Iorio R, Pietrocola F, Einer C, Borchard S, Zibert A, Schmidt HH, Di Schiavi E, Puchkova LV, Franco B, Kroemer G, Zischka H and Polishchuk RS. Activation of autophagy, observed in liver tissues from patients with Wilson disease and from ATP7B-deficient animals, protects hepatocytes from copper-induced apoptosis. Gastroenterology 2019; 156: 1173-1189, e1175.
[10] Wang Y, Shen J, Xiong X, Xu Y, Zhang H, Huang C, Tian Y, Jiao C, Wang X and Li X. Remote ischemic preconditioning protects against liver ischemia-reperfusion injury via heme oxygenase-1-induced autophagy. PLoS One 2014; 9: e98834.
[11] Li J, Zhou J, Zhang D, Song Y, She J and Bai C. Bone marrow-derived mesenchymal stem cells enhance autophagy via PI3K/AKT signalling to reduce the severity of ischaemia/reperfusion-induced lung injury. J Cell Mol Med 2015; 19: 2341-2351.
[12] Wang X, Li C, Wang Q, Li W, Guo D, Zhang X, Shao M, Chen X, Ma L, Zhang Q, Wang W and Wang Y. Tanshinone IIA restores dynamic balance of autophagosome/autolysosome in doxorubicin-induced cardiotoxicity via targeting beclin1/LAMP1. Cancers (Basel) 2019; 11.
[13] Wu WY, Wang WY, Ma YL, Yan H, Wang XB, Qin YL, Su M, Chen T and Wang YP. Sodium tanshinone IIA silate inhibits oxygen-glucose deprivation/recovery-induced cardiomyocyte apoptosis via suppression of the NF-kappaB/TNF-alpha pathway. Br J Pharmacol 2013; 169: 1058-1071.
[14] Jang SI, Kim HJ, Kim YJ, Jeong SI and You YO. Tanshinone IIA inhibits LPS-induced NF-kappaB activation in RAW 264.7 cells: possible involvement of the NIK-IKK, ERK1/2, p38 and JNK pathways. Eur J Pharmacol 2006; 542: 1-7.
[15] Ko JS, Ryu SY, Kim YS, Chung MY, Kang JS, Rho MC, Lee HS and Kim YK. Inhibitory activity of diacylglycerol acyltransferase by tanshinones from the root of Salvia miltiorrhiza. Arch Pharm Res 2002; 25: 446-448.
[16] Zhou L, Bondy SC, Jian L, Wen P, Yang F, Luo H, Li W and Zhou J. Tanshinone IIA attenuates the cerebral ischemic injury-induced increase in levels of GFAP and of caspases-3 and -8. Neuroscience 2015; 288: 105-111.
[17] Yun SM, Jung JH, Jeong SJ, Sohn EJ, Kim B and Kim SH. Tanshinone IIA induces autophagic cell death via activation of AMPK and ERK and inhibition of mTOR and p70 S6K in KBM-5 leukemia cells. Phytother Res 2014; 28: 458-464.
[18] Chang M, Lu S, Zhang F, Zuo T, Guan Y, Wei T, Shao W and Lin G. RGD-modified pH-sensitive liposomes for docetaxel tumor targeting. Colloids Surf B Biointerfaces 2015; 129: 175-182.
[19] Wang S, Hossack JA and Klibanov AL. Targeting of microbubbles: contrast agents for ultrasound molecular imaging. J Drug Target 2018; 26: 420-434.
[20] Kono K, Nakashima S, Kokuryo D, Aoki I, Shimomoto H, Aoshima S, Maruyama K, Yuba E, Kojima C, Harada A and Ishizaka Y. Multifunctional liposomes having temperature-triggered release and magnetic resonance imaging for tumor-specific chemotherapy. Biomaterials 2011; 32: 1387-1395.
[21] Yang W, Yu XC, Chen XY, Zhang L, Lu CT and Zhao YZ. Pharmacokinetics and tissue distribution profile of icariin propylene glycol-liposome intraperitoneal injection in mice. J Pharm Pharmacol 2012; 64: 190-198.
[22] Hu C, Liang K, An R, Wang X and You L. The characterization, pharmacokinetic, and tissue distribution studies of TPGS-modified artesunate liposome in rats. Drug Dev Ind Pharm 2018; 44: 1528-1535.
[23] Zhang J, Liang H, Yao H, Qiu Z, Chen X, Hu X, Hu J and Zheng G. The preparation, characterization of Lupeol PEGylated liposome and its functional evaluation in vitro as well as pharmacokinetics in rats. Drug Dev Ind Pharm 2019; 45: 1052-1060.
[24] Liu Y, Sun C, Li W, Adu-Frimpong M, Wang Q, Yu J and Xu X. Preparation and characterization of syringic acid-loaded TPGS liposome with enhanced oral bioavailability and in vivo antioxidant efficiency. AAPS PharmSciTech 2019; 20: 98.
[25] Hu H, Zhai C, Qian G, Gu A, Liu J, Ying F, Xu W, Jin D, Wang H, Hu H, Zhang Y and Tang G.

Protective effects of tanshinone IIA on myocardial ischemia reperfusion injury by reducing oxidative stress, HMGB1 expression, and inflammatory reaction. Pharm Biol 2015; 53: 1752-1758.
[26] Liang P, Zheng J, Zhang Z, Hou Y, Wang J, Zhang C and Quan C. Bioactive 3D scaffolds self-assembled from phosphorylated mimicking peptide amphiphiles to enhance osteogenesis. J Biomater Sci Polym Ed 2019; 30: 34-48.
[27] Feng Y, He Z, Mao C, Shui X and Cai L. Therapeutic effects of resveratrol liposome on muscle injury in rats. Med Sci Monit 2019; 25: 2377-2385.
[28] Shi ZR, Itzkowitz SH and Kim YS. A comparison of three immunoperoxidase techniques for antigen detection in colorectal carcinoma tissues. J Histochem Cytochem 1988; 36: 317-322.
[29] Ozkan F, Senayli Y, Ozyurt H, Erkorkmaz U and Bostan B. Antioxidant effects of propofol on tourniquet-induced ischemia-reperfusion injury: an experimental study. J Surg Res 2012; 176: 601-607.
[30] Tang LM, Wang LX, Wang ZY, Sun LF, Pan XD and Pan GQ. Tanshinone IIA ameliorates lead (Pb)-induced cognitive deficits and oxidative stress in a rat pup model. Bratisl Lek Listy 2017; 118: 196-201.
[31] Yang GL, Jia LQ, Wu J, Ma YX, Cao HM, Song N and Zhang N. Effect of tanshinone IIA on oxidative stress and apoptosis in a rat model of fatty liver. Exp Ther Med 2017; 14: 4639-4646.
[32] Wang D, Liu Y, Zhong G, Wang Y, Zhang T, Zhao Z, Yan X and Liu Q. Compatibility of Tanshinone IIA and Astragaloside IV in attenuating hypoxia-induced cardiomyocytes injury. J Ethnopharmacol 2017; 204: 67-76.
[33] Chen X, Wu R, Kong Y, Yang Y, Gao Y, Sun D, Liu Q, Dai D, Lu Z, Wang N, Ge S and Wang F. Tanshinone IIA attenuates renal damage in STZ-induced diabetic rats via inhibiting oxidative stress and inflammation. Oncotarget 2017; 8: 31915-31922.
[34] Omari-Siaw E, Wang Q, Sun C, Gu Z, Zhu Y, Cao X, Firempong CK, Agyare R, Xu X and Yu J. Tissue distribution and enhanced in vivo anti-hyperlipidemic-antioxidant effects of perillaldehyde-loaded liposomal nanoformulation against Poloxamer 407-induced hyperlipidemia. Int J Pharm 2016; 513: 68-77.
[35] Mellins ED. The role of the MHC in autoimmunity: an overview. J Rheumatol Suppl 1992; 33: 63-69.
[36] Zamoner A, Barreto KP, Filho DW, Sell F, Woehl VM, Guma FC, Silva FR and Pessoa-Pureur R. Hyperthyroidism in the developing rat testis is associated with oxidative stress and hyperphosphorylated vimentin accumulation. Mol Cell Endocrinol 2007; 267: 116-126.
[37] Chapman MA, Zhang J, Banerjee I, Guo LT, Zhang Z, Shelton GD, Ouyang K, Lieber RL and Chen J. Disruption of both nesprin 1 and desmin results in nuclear anchorage defects and fibrosis in skeletal muscle. Hum Mol Genet 2014; 23: 5879-5892.
[38] Arnardottir S, Borg K and Ansved T. Sporadic inclusion body myositis: morphology, regeneration, and cytoskeletal structure of muscle fibres. J Neurol Neurosurg Psychiatry 2004; 75: 917-920.
[39] Dekkers BG, Spanjer AI, van der Schuyt RD, Kuik WJ, Zaagsma J and Meurs H. Focal adhesion kinase regulates collagen I-induced airway smooth muscle phenotype switching. J Pharmacol Exp Ther 2013; 346: 86-95.
[40] Criswell TL, Corona BT, Ward CL, Miller M, Patel M, Wang Z, Christ GJ and Soker S. Compression-induced muscle injury in rats that mimics compartment syndrome in humans. Am J Pathol 2012; 180: 787-797.
[41] Kim JT, Kasukonis BM, Brown LA, Washington TA and Wolchok JC. Recovery from volumetric muscle loss injury: a comparison between young and aged rats. Exp Gerontol 2016; 83: 37-46.
[42] Ferrando AA. Effects of inactivity and hormonal mediators on skeletal muscle during recovery from trauma. Curr Opin Clin Nutr Metab Care 2000; 3: 171-175.
[43] Wang L, Shan Y, Chen L, Lin B, Xiong X, Lin L and Jin L. Colchicine protects rat skeletal muscle from ischemia/reperfusion injury by suppressing oxidative stress and inflammation. Iran J Basic Med Sci 2016; 19: 670-675.
[44] Pattwell D, McArdle A, Griffiths RD and Jackson MJ. Measurement of free radical production by in vivo microdialysis during ischemia/reperfusion injury to skeletal muscle. Free Radic Biol Med 2001; 30: 979-985.
[45] Raghavan S, Subramaniyam G and Shanmugam N. Proinflammatory effects of malondialdehyde in lymphocytes. J Leukoc Biol 2012; 92: 1055-1067.
[46] He F, Li J, Liu Z, Chuang CC, Yang W and Zuo L. Redox mechanism of reactive oxygen species in exercise. Front Physiol 2016; 7: 486.
[47] Sirota TV, Zakharchenko MV and Kondrashova MN. Cytoplasmic superoxide dismutase activity is a sensitive indicator of the antioxidant status of the rat liver and brain. Biomed Khim 2014; 60: 63-71.
[48] Wang FY, Jia J, Song HH, Jia CM, Chen CB and Ma J. Icariin protects vascular endothelial cells from oxidative stress through inhibiting endoplasmic reticulum stress. J Integr Med 2019; 17: 205-212.